J Fluoresc (2012) 22:815–825
DOI 10.1007/s10895-011-1016-y

ORIGINAL PAPER

Spectral and Photophysical Properties of α-carboline (1-Azacarbazole) in Aqueous Solutions

Emilio García-Fernández · Carmen Carmona · María A. Muñoz · José Hidalgo · Manuel Balón

Received: 18 July 2011 / Accepted: 21 November 2011 / Published online: 7 December 2011

Abstract The absorption and fluorescence spectra of α-carboline, 9H-pyrido[2,3-b]indole, AC, in organic aprotic solvents containing different water proportions and in acid/base aqueous solutions inside and outside the pH range have been examined. In the organic aprotic solvents, the addition of increasing concentrations of water sequentially quenches and shifts to the red the fluorescence spectra of AC. These spectral changes have been rationalized assuming the formation, at the lower water concentrations, of a discrete ground state non-cyclic weakly fluorescent AC hydrate emitting at 376 nm that, upon increasing the water concentrations, evolves to a higher order AC poly hydrate emitting at 397 nm. The changes of the AC absorption spectra in aqueous acid/basic solutions indicate the existence of three ground state prototropic species; the pyridinic protonated cation, C (pK_a=4.10±0.05), the neutral, N (pK_a=14.5±0.2), and the pyrrolic deprotonated anion, A. Conversely, the changes of the AC fluorescence spectra in these media indicate the existence of four excited state species emitting at 376 nm, 397 nm, 460 nm and 465 nm. Since the emissions at 376 nm and 397 nm satisfactorily match those of the hydrates observed in the organic-water mixtures, they were consistently assigned to two differently hydrated ground state N species. The remaining emissions at 460 nm and 465 nm have been assigned without ambiguity, on the basis of their excitation spectra, to the C and A species, respectively. The excited-state pK_as of the prototropic species of AC have been estimated by using the Förster-Weller cycle.

Keywords α-carboline · Prototropic equilibria · Hydrates · Photophysics · Aqueous media

E. García-Fernández · C. Carmona · M. A. Muñoz · J. Hidalgo · M. Balón (✉)
Departamento de Química Física, Facultad de Farmacia, Universidad de Sevilla,
41012 Sevilla, Spain
e-mail: balon@us.es

Introduction

The apparently anomalous photophysical behavior of the 7-Azaindole, 7AI, in water has long attracted considerable interest [1, 2]. As it is well known, in hydrocarbon and alcohol solvents, 7AI forms cyclic doubly hydrogen-bonded dimers and solute/solvent complexes, respectively. Upon photoexcitation, these complexes undergo a concerted intermolecular excited state double proton transfer, ESDPT, reaction. As a result, the room temperature fluorescence spectrum of the 7AI solutions in these solvents shows dual emissions with short and long wavelength bands attributed to the 7AI monomer or the 7AI/alcohol complexes and to their phototautomerized species, respectively. In contrast, 7AI in water exhibits only a single fluorescence band at 385 nm that shows double exponential fluorescence decays and growths.

Although the origin of this band has been the subject of conflicting interpretations [3–9], it is generally accepted that the photophysics of 7-azaindole in water is mainly dominated by 7AI hydrates [5, 7] that, because of their 'blocked' structures for the ESDPT process, are unable to phototautomerize. However, a very small fraction of cyclic doubly hydrogen bonded 7AI monohydrates, possessing an appropriate hydrogen-bonded structure, are able to phototautomerize directly and rapidly, just as in the case of the dimer. This assumption was supported by the fact that, upon the addition of small quantities of water to the 7AI solutions

in aprotic solvents, the green fluorescence attributable to the phototautomer of the 7AI monohydrate can be easily observed [5]. Thus, according to these authors, [7], in bulk water the weak long wavelength fluorescence of these phototautomers is hidden under the red edge of the main emission band.

α-carboline, or 1-azacarbazole, AC, Scheme 1, is another representative diaza-aromatic molecule that can experience an ESDPT process and phototautomerism. Because of its structural relation with 7AI, the photophysics of AC has received outstanding attention [10–20]. Thus, it has been reported that AC forms, similarly to 7AI, cyclic doubly hydrogen-bonded dimers and solute/solvent complexes in hydrocarbon and alcoholic solvents, respectively. Upon photoexcitation, these species promote the AC phototautomerism undergoing an ESDPT process and emitting dual fluorescence. In bulk water, AC also shows the apparently anomalous photophysical behavior of 7AI [10, 13, 19]. Consequently, it has been presumed that AC also forms cyclic doubly hydrogen bonded monohydrates similar to those of 7AI. However, the experimental evidences supporting this presumption have not been reported. In fact, the photophysical behavior of AC in aqueous media has been scarcely studied and the published data on this system are scattered among the different papers devoted to the AC photophysics. Moreover, although some years ago, in the context of a theoretical study on the acid–base properties of the carbolines, we reported the ground state pK_as of AC, the spectral data used to obtain these pK_as were not even included in this paper [21].

Therefore, to get a better understanding of the AC photophysics in water, we have thought interesting to systematically study the spectral and photophysical properties of AC in aqueous media. The main goal of this study is to spectroscopically characterize the ground and excited state prototropic species of AC and to discern the nature of the AC hydrates that could be present in neutral aqueous solutions. For this purpose, we have analyzed the influence of acids, bases and water addition on the absorption and fluorescence spectra of aqueous and organic AC solutions, respectively.

Experimental

AC was synthesized and purified as described elsewhere [22]. Citric acid and sodium di-hydrogen phosphate used for the buffer solutions, HCl and NaOH were analytical grade commercial products of the best available quality (≥95%, Sigma-Aldrich) and were used without further purification. Doubly distilled water was used thoroughly. The pHs of the buffer solutions were measured with a Radiometer Copenhagen PMH80 pH-meter and a Teknokroma Single Pore Glass P/N 238160 electrode. Spectral grade organic solvents diethyl ether, DEE, tetrahydrofurane, THF, and dioxane, DX, of the highest available purity were freshly prepared and used as received. Non-degassed solutions for spectroscopic measurements were freshly prepared and kept in the dark to avoid photodecomposition.

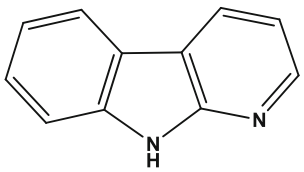

Scheme 1 α-carboline, 9H-pyrido[2,3-b]indole, AC

The UV–vis absorption spectra were recorded on a Cary 100 spectrophotometer and the stationary fluorescence measurements in a pre-calibrated Hitachi F-2500 spectrofluorimeter using Spectrosil quartz cells of 1 cm path length. Dilute solutions of AC (≈10^{-5} M) were used to avoid inner filter effects and re-absorption phenomena. The Peak Fit© Jandel Scientific Program was used to re-convolute the experimental fluorescence spectra of AC in DX-water mixtures from their individual components. The emission bands were fitted to the logistic symmetric function:

$$y = a_0(1+\exp X)^{-(a_3+1)} a_3{}^{-a_3}(a_3+1)^{(a_3+1)} \exp X \qquad (1)$$

with

$$X = -\frac{(x + a_2 \ln a_3 - a_1)}{a_2} \qquad (2)$$

The amplitudes, a_0, centres, a_1, widths, a_2, and shapes, a_3 of the convoluted bands were optimised with the Marquardt algorithm. The goodness of the fits was judged by the correlation coefficient and the visual inspection of the residuals.

The time-resolved fluorescence measurements were performed with the time-correlated single photon counting FL900CD and Mini-τ spectrofluorimeters of Edinburgh Analytical Instruments. These instruments used as the excitation sources a nF900 hydrogen flash lamp and a Pico-Quant laser diode, respectively. The fluorescence decay curves were acquired to (1–2) 10^4 counts in the peak and were fitted, by re-convolution analysis with the instrumental response function, to a sum of exponential functions with amplitudes, α_i, and lifetimes, τ_i.

$$I(t) = \sum \alpha_i \exp(-t/\tau_i) \qquad (3)$$

The quality of the fits was analysed by the randomness of the residuals and the reduced chi-squares (χ^2). Global analyses of the fluorescence decays were performed using the standard program Level 2 based on the tried and tested Marquardt-Levenberg algorithm, supplied by Edinburgh Analytical Instruments.

Results and Discussion

Spectral Characterization of the AC Hydrates in the Water-Organic Mixtures

As stated in the Introduction, one of the main goals of this study is to look for the AC hydrates that could be present in bulk water and to investigate their nature and photophysics properties. For this purpose, we have examined the influence of water addition on the absorption and fluorescence spectra of AC in different water miscible aprotic solvents. After this previous scrutiny, we have selected DX, THF and DEE as the more representative solvents to illustrate the characteristics of these spectral changes.

Upon water addition, the structured low energy absorption band in the absorption spectrum of a 1 10^{-4} M solution of AC in DX broadens and shifts slightly to the red, Fig. 1. The fluorescence spectrum of this AC solution diminishes in intensity, loses its vibrational structure, broadens and progressively shifts to the red practically matching, at the higher water concentrations, the fluorescence emission spectrum of AC in bulk water, Fig. 2. This behaviour resembles that previously reported for 7AI in these organic solvent-water mixtures [5], but with an important difference: the distinctive long emission band that would be attributable to the cyclic double hydrogen bonded AC monohydrates is not observed. Therefore, this intriguing result suggests that, unlike 7AI, AC does not form the 1:1 cyclic hydrogen bonded AC/water complex structurally ready for a rapid ESDPT process depicted in Scheme 2.

The absence of isosbestic and isoemissive points in the absorption and fluorescence spectra of AC in the DX-water mixtures, suggests that AC hydrogen bond to water molecules forming a variety of AC hydrates. However, despite the apparent complexity of this system, the Stern-Volmer plot, in the inset of Fig. 2, of the ratio of the areas, A_0/A, under the emission spectra of the AC solutions in DX before, A_o, and after, A, the water addition, against the water concentration surprisingly shows well defined straight lines at the lower and the higher water concentrations, respectively. This behaviour points out that, at least, two different types of hydrates are responsible for the changes of the AC fluorescence spectra. In this regard, it is worth noting that the experimental fluorescence spectra of AC in the DX-water mixtures can be excellently reproduced by re-convoluting two emissions bands centered at 376 nm and 397 nm, Fig. 3. Interestingly, the contributions of these bands decrease and increase, respectively, as the water concentration increases. These results confirm that the AC-water hydrogen bonding interactions take place sequentially and involve two different species.

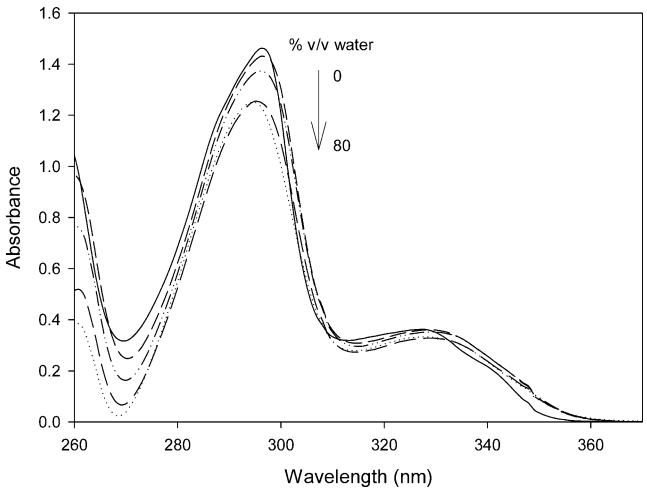

Fig. 1 Influence of water addition (% v/v) on the absorption spectrum of a 1 10^{-4} M solution of AC in DX

The results obtained in THF plentifully support this hypothesis. Thus, upon the addition of small water concentrations, the fluorescence spectrum of AC in this solvent loses its vibrational structure and its intensity is strongly quenched, Fig. 4. However, once this initial quenching process has been practically completed, the further increase of water concentration shifts markedly to the red the AC fluorescence spectrum. The addition of water also produces similar, but even more pronounced, quenching of the AC fluorescence in DEE (spectra not shown). However, due to the limited solubility of water in this solvent, the higher water concentrations necessary to observe the expected further red shift of the fluorescence spectrum could not be achieved. These results suggest that the quenching and the red shift of the AC fluorescence spectra in the organic-water media have different origins. Because, as mentioned, the spectral changes in the THF-water mixtures take place in well separate ranges of water concentrations, we will take this advantage to get a further insight on the nature of these phenomena.

In the range of the low water concentrations where the quenching of the AC fluorescence is observed, the Stern-Volmer plot of the ratio of the areas, A_0/A, under the emission spectra of the AC solutions in THF, before, A_o, and after, A, the water addition, against the water concentration shows a negative deviation typical of inhomogeneous ground state systems, inset of Fig. 4. Accordingly, the fluorescence of these solutions shows bi-exponential decays. Global analysis of these decays gives constant lifetimes around ~7 ns, close to that of AC in pure THF (7.43± 0.04 ns), and ~3 ns. The relative contributions of these lifetimes to the emission decrease and increase upon increasing the water concentration, respectively. These results can be reasonably explained assuming the ground state formation of a weakly fluorescent hydrogen bonded AC/$(H_2O)_n$ complex emitting around 376 nm. Moreover, the time resolved fluorescence data indicate that the free AC

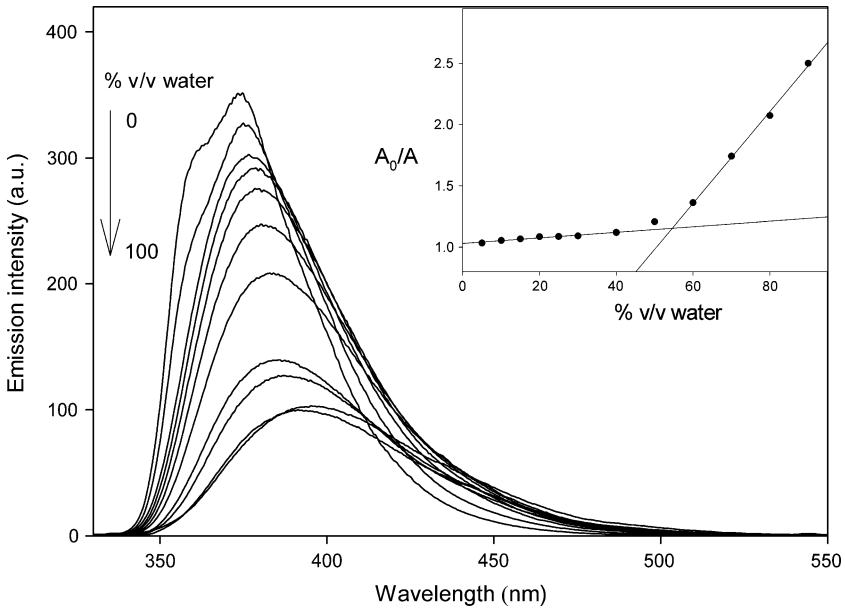

Fig. 2 Influence of water addition (% v/v) on the fluorescence spectrum of a 2 10^{-5} M solution of AC in DX, λ_{exc}=298 nm. In the inset: Stern-Volmer plot of the ratio of the areas, A_0/A, under the emission spectra against the water concentration

molecule and the AC/$(H_2O)_n$ complex behave as independent fluorophores; namely, they do not interconvert in the singlet excited state, Scheme 3.

According to the proposed model, the ground state formation of the AC/$(H_2O)_n$ complex in the THF-water mixtures can be expressed as:

$$AC + nH_2O \rightleftarrows AC/(H_2O)_n \tag{4}$$

being the apparent equilibrium constant, K_C:

$$K_C = \frac{[AC/(H_2O)_n]}{[AC][H_2O]^n} \tag{5}$$

Taking logarithms and rearranging we obtain:

$$\ln \frac{[AC/(H_2O)_n]}{[AC]} = \ln K_C + n \ln[H_2O] \tag{6}$$

Finally, assuming that the fluorescence spectra is composite of the emissions of the non-hydrated and hydrated AC species and that their intensities are proportional to their ground state concentrations, a straightforward derivation lets us to transform the Eq. (6) in the following equation:

$$\ln \frac{A_0 - A}{A - A_\infty} = \ln K_C + n \ln[H_2O] \tag{7}$$

where A_0 and A have the same significance as before and A_∞ represents the integrated intensity of the AC fluorescence spectrum once the AC/$(H_2O)_n$ complex has been completely formed. As Fig. 5a shows, the plot of the fluorescence data according to Eq. (7) gives a straight line. The value obtained for n from the slope of this plot, 1.8±0.2, suggests that this complex has the structure of the AC/$(H_2O)_2$ complex depicted in Scheme 2. On the other hand, from the intercept of this plot, a value of 8.4±0.4 M^{-2} can be estimated for the formation constant, K_C, of this complex. The analysis of the fluorescence data of AC in the

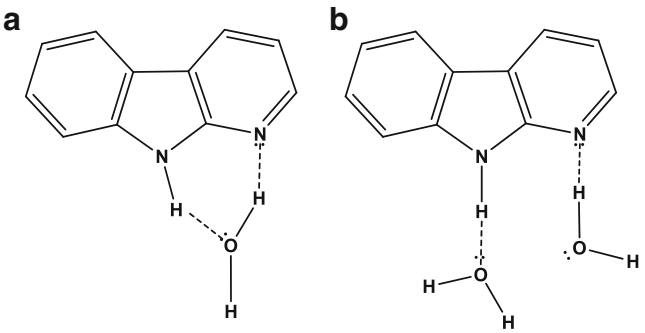

Scheme 2 Doubly hydrogen bonded 1:1 (**a**) and 1:2 AC-water complexes

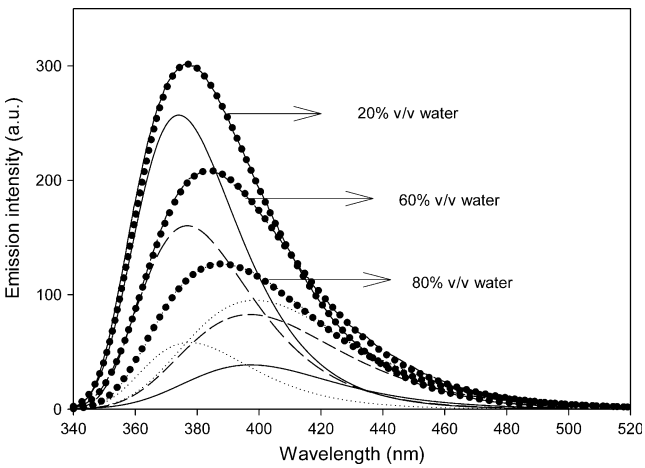

Fig. 3 Experimental (*bold*) and re-convoluted (*circles*) fluorescence spectra of AC in some representative DX-water mixtures

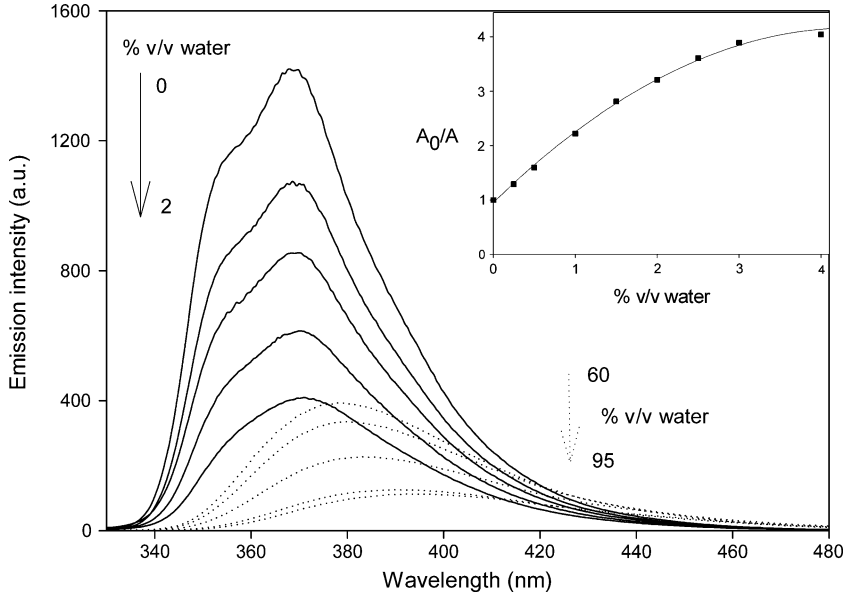

Fig. 4 Influence of water addition (% v/v) on the fluorescence spectra of a 2 10^{-5} M solution of AC in THF, λ_{exc}=298 nm. In the inset: Stern-Volmer plot of the ratio of the areas, A_0/A, under the emission spectra of the AC solutions in THF against the water concentration

DEE-water mixtures gives similar results but, possibly due to the lower polarity of this solvent, the value obtained for the formation constant K_C, 58±5 M^{-2} is greater than that obtained in THF.

After this initial quenching process, the further increase of the water concentrations progressively shifts to the red and diminishes the intensity of the fluorescence spectrum of AC in the THF-water mixtures. In these media, the AC fluorescence decays mono-exponentially with lifetimes close to that of AC in bulk water, ~2.5 ns. As in the water-poor mixtures, the analysis of the steady-state fluorescence data of the water-rich mixtures according to Eq. (7), taking now for A_0 the value of A_∞ corresponding to the complete formation of the AC/$(H_2O)_2$ complex, yields also a straight line but with a greater slope, 5.7±0.3, Fig. 5b. This result points out to the formation of a new AC/water hydrate with a higher number of water molecules. Because of the property of the water molecules to accommodate up to four hydrogen bonds, we suppose that the primary solvation shell of this hydrate would involve a water cluster with extensive hydrogen bonding between the water molecules. To test this hypothesis we have examined the influence of the tert-butanol, tButOH, addition on the spectra of AC in hexane. We have selected this alcohol because its molecular structure is little prone to self-aggregation.

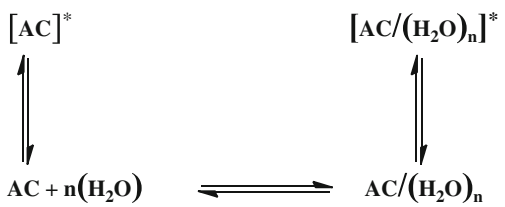

Scheme 3 Hydrogen bonding interaction between AC and H_2O

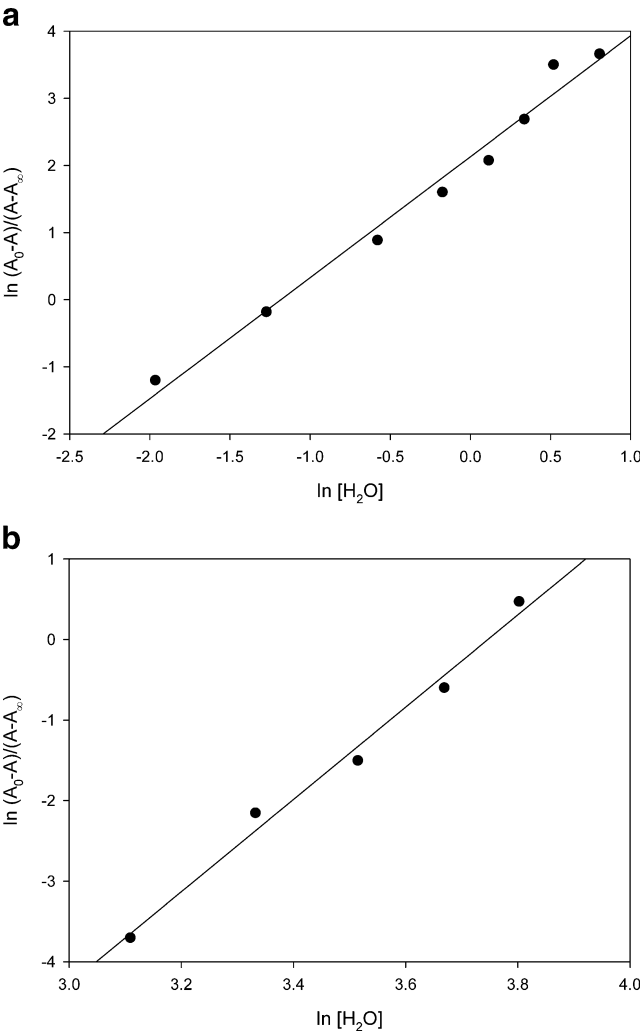

Fig. 5 Plots according to Eq. (7) of the steady state fluorescence data of the AC solutions in water-poor (**a**) and water-rich (**b**) THF-water mixtures

The spectra reported in Fig. 6 clearly support this presumption. Thus, the addition of tButOH induces changes in the absorption spectrum of AC similar to those produced by water. However, it must be noted that the spectra of the AC-tButOH system have clearly defined isosbestic points not observed in the AC-water spectra. These results show that, differently as for water occurs, tButOH only forms one hydrogen-bonded complex with AC. The formation of this AC-tButOH complex also quenches and slightly shifts to the red the fluorescence spectrum of AC, inset of Fig. 6. Therefore, as we presumed, once the AC-tButOH complex has been completely formed, because of the difficulty of the t-ButOH molecules to self-aggregate, the fluorescence spectrum of the AC-tButOH mixtures does not experience further changes. This spectrum is very close to that of AC in pure tButOH, which, possibly due to solvatochromic effects, is less structured and slightly red shifted (λ_{max} ~371 nm). Noteworthy, the long emission band that would be attributable to the 1:1 cyclic double hydrogen bonded AC-tButOH complexes is neither observed in this system.

Spectral Characterization of the Prototropic Species of AC in Aqueous Solutions

Due to the presence in its structure of a moderately basic pyridinic nitrogen atom and a weakly acid pyrrolic group, AC is expected to show an amphoteric behavior in aqueous solutions, being protonated in moderately acid media (inside the pH range) and deprotonated in highly basic solutions (outside the pH range), Scheme 4. Accordingly, we have systematically examined the absorption spectra of AC in buffered and NaOH solutions, Fig. 7. The changes observed in these spectra show the expected ground state equilibria between the neutral, N, cationic, C, and anionic, A, prototropic species of AC depicted in Scheme 4.

As illustrated in this Figure, upon protonation and deprotonation of N to form C and A species, the low energy band of the absorption spectrum shifts to the red around 15 nm and 45 nm, respectively. The analysis of the spectrophotometric titration data by using the classical Henderson-Hasselbach equation [23] (inside the pH range) and the Excess Acidity Function method [24] (outside the pH range) renders pK_a values of 4.10±0.05 and 14.5±0.2 for the C→N and N→A prototropic equilibria, respectively. These pK_a values, in good agreement with those previously reported by others authors and ourselves [13, 21], are similar to those published for 7AI (4.5±0.1 and 12.1, respectively) [8]. On the other hand, these pK_as values indicate that while the pyridinic nitrogen atom of AC is the less basic of the four isomers of the carboline ring, the acidity of the pyrrolic proton is similar within the carboline family [21].

The fluorescence spectra obtained by exciting the AC solutions in the 0–10 pH range at the isosbestic point of the absorption spectra, reveal the presence of two emitting species, Fig. 8a. At the lower pHs, the AC solutions emit around 460 nm and, at moderately acid, neutral, and moderately basic pHs, around 397 nm. Under these experimental conditions, the emission decays of the AC solutions, excited at the isosbestic point, are characterized by only one lifetime in acid (pH<2) and neutral (pH 6–8) media, ~0.9 ns and ~2.5 ns, respectively, and by some combination of these two lifetimes at intermediate pHs. As the basicity of the AC solutions increases above pH≈10, the intensity of the emission at 397 nm strongly diminishes. Moreover, in the concentrated NaOH solutions (~2–8 M), the fluorescence spectra of AC show double emissions with very weak bands at 376 nm and

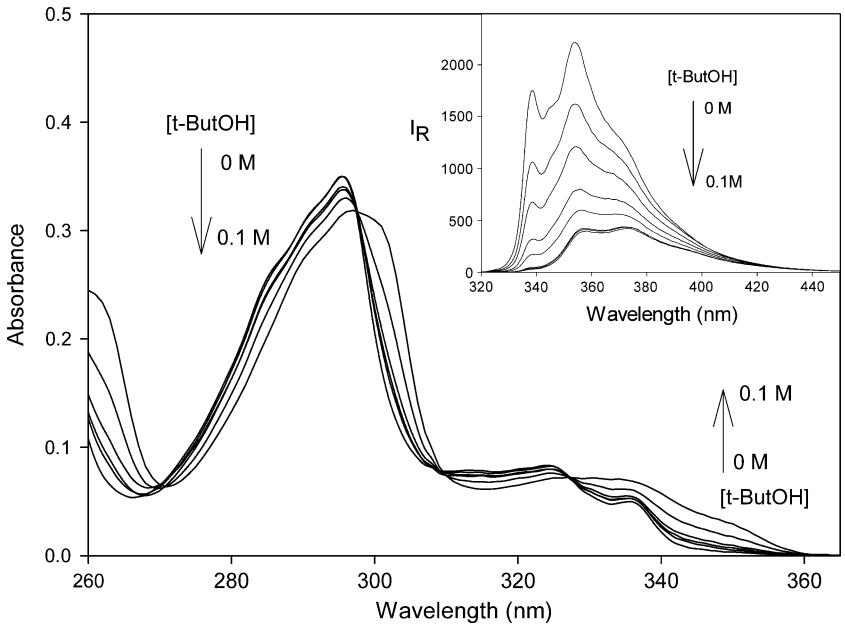

Fig. 6 Influence of tButOH addition on the absorption spectrum of a 2 10^{-5} M solution of AC in hexane. In the inset, influence of tButOH addition on the fluorescence spectrum of a 2 10^{-5} M solution of AC in hexane

Scheme 4 Ground state prototropic equilibria of AC

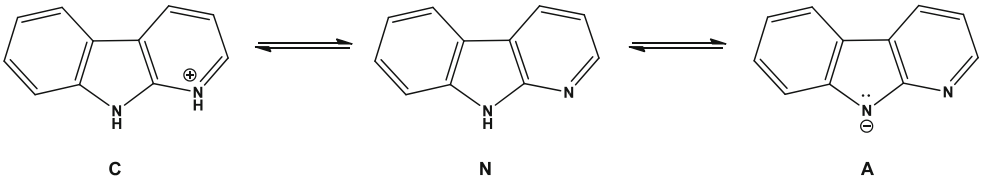

465 nm whose intensities decrease and increase, respectively, as the concentration of the NaOH solutions increases, Fig. 8b. Unfortunately, the extremely low intensities of these fluorescence emissions precluded a detailed study of the dynamic of the system in these media. Finally, in highly concentrated solutions of NaOH (~11 M), the band at 465 nm is the only emission observed in the fluorescence spectrum of AC, Fig. 8b. This band decays mono-exponentially with a lifetime of ~6 ns.

The analysis of the acid/base influence on the fluorescence spectra of AC reveals the existence of four different emissions at 376 nm, 397 nm, 460 nm and 465 nm. The normalized fluorescence spectra showing these representative emissions are recorded in Fig. 9. Noteworthy, the fluorimetric titration plots in the inset of Fig. 8a and b of the fluorescence intensities measured at 397 nm and 465 nm indicate that the excited-state emissions reflect the underlying ground state C→N and N→A equilibria, respectively. Therefore, these results suggest that these equilibria are not apparently established during the singlet excited-state lifetimes of the AC prototropic species.

Noteworthy, the emission bands at 460 nm and 465 nm are practically coincident. However, because of the disparate media where they are obtained, they would not reasonably proceed from the same ground state precursor. In fact, their different excitation spectra (not shown) closely reproduce the absorption spectra of the ground state species predominating in the media where they are observed. Therefore, these bands at 460 nm and 465 nm can be unambiguously assigned to the emissions of C and A, respectively. Accordingly, AC excellently accomplishes the Valle-Kasha-Catalán rule: "*In a diheterocyclic aromatic molecule with proton-acceptor and proton-donor heteroatom systems, a coincidence or near coincidence of the corresponding cation and anion fluorescence bands will be manifested*" [25].

The remaining emissions at 376 nm and 397 nm have similar excitation spectra. Since these spectra roughly resemble the absorption spectrum of the N species, we can conclude that N is the common ground state precursor for both emissions. Interestingly, there is a close correspondence between these bands and those of the fluorescence spectra of AC in the organic-water mixtures attributed to the AC/$(H_2O)_2$ complex and the AC poly-hydrates. Thus, as the normalized spectra in Fig. 10 show, the band at 376 nm of the AC spectrum in NaOH 5.6 M, reasonably matches that observed in the emission spectrum of AC in THF with a 10% v/v of water content. On the other hand, the emissions around 397 nm observed in moderately acid or basic and in neutral media and the emission observed in the spectrum of AC in THF with a 95% v/v of water content are practically coincident.

According to these results the emissions at 397 nm and 376 nm can be assigned to two differently hydrated neutral AC species. Concretely, the hydration of the neutral species emitting around 397 nm in moderately acid and basic aqueous media should be close to that of the AC poly hydrates predominating in the organic-water mixtures with high water concentrations. Similarly, the hydrated structure of the neutral

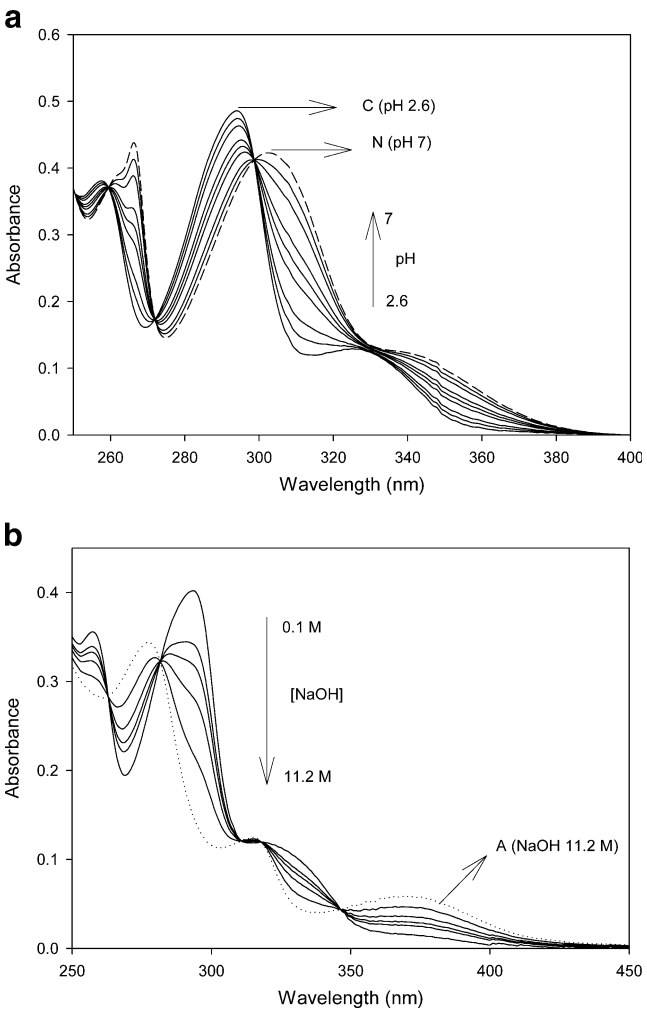

Fig. 7 Absorption spectra of 2 10^{-5} M solutions of AC in buffered (**a**) and NaOH (**b**) aqueous solutions

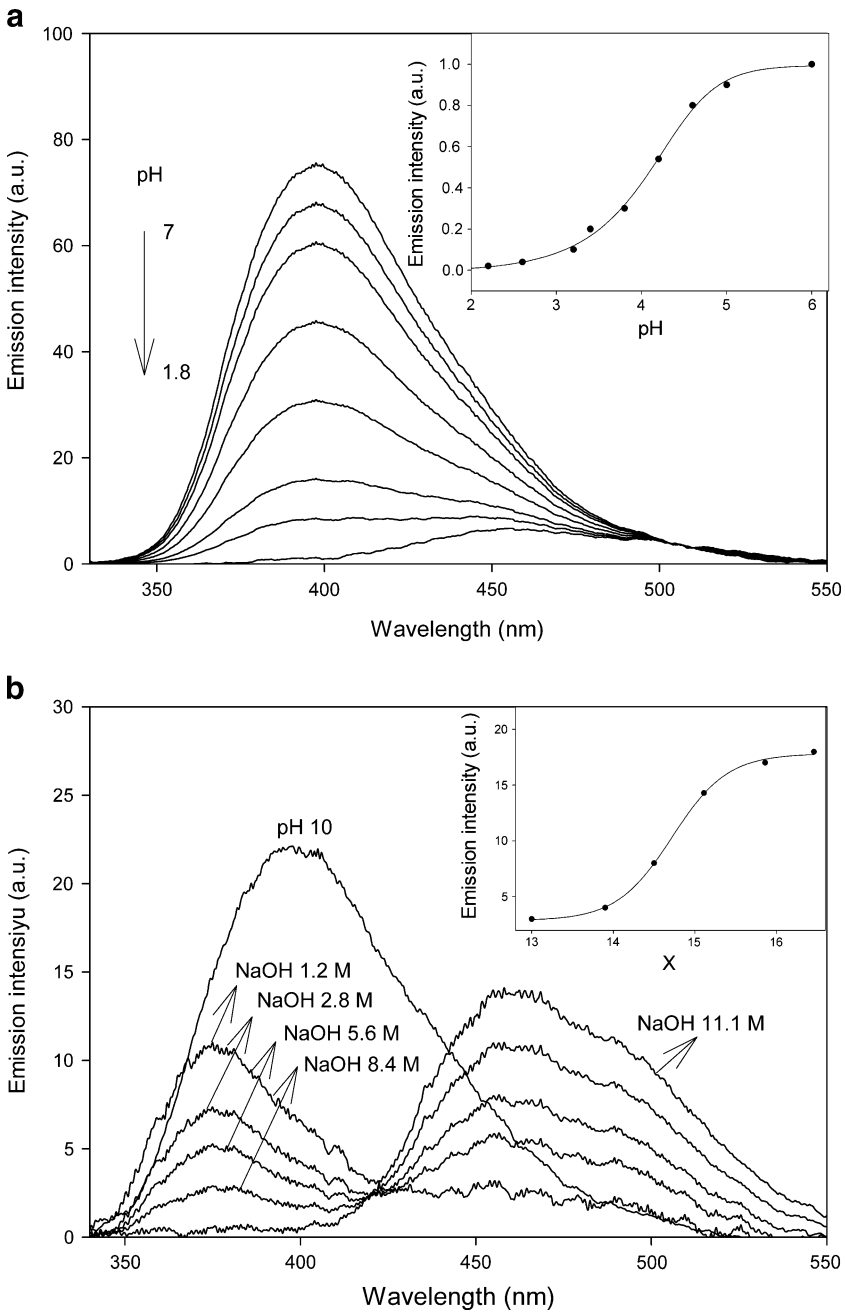

Fig. 8 Fluorescence spectra of 2 10^{-5} M solutions of AC in buffered (**a**) and NaOH (**b**) aqueous solutions, λ_{exc}= 302 nm. In the insets, the fluorimetric titration plots of the normalized fluorescence intensities measured at (**a**) 397 nm and (**b**) 465 nm

species emitting at 376 nm in moderately concentrated NaOH solutions should be similar to that of the AC-$(H_2O)_2$ complex formed in the organic-water mixtures with low water concentrations. Therefore, it seems that the neutral AC molecule undergoes a dehydration process on going from the moderately buffered acidic media to the strong basic aqueous solutions. Evidently, the increasing concentration of the OH^- ions must play a key role in this "drying" process.

The proposed hydration/dehydration processes of the AC-water complexes remind a similar phenomenon previously observed in the water assisted proton transfer reactions of the 9-methylbetacarboline, MBC [26, 27]. Thus, we have recently shown that the ground and the excited state pyridinic protonation of MBC in N,N-dimethylformamide-water mixtures requires the sequential formation of MBC-water hydrates upon increasing the number of water molecules [26]. Conversely, the reverse excited state deprotonation reaction involves the dehydration, in highly concentrated NaOH aqueous solutions, of the strongly hydrated MBC cations [27]. These results point out that, as observed in other similar reactions, the formation of water clusters in the hydration sphere of the organic molecules is a fundamental condition for the proton transfer processes [28–34]. The cooperative hydrogen bonding among the water molecules

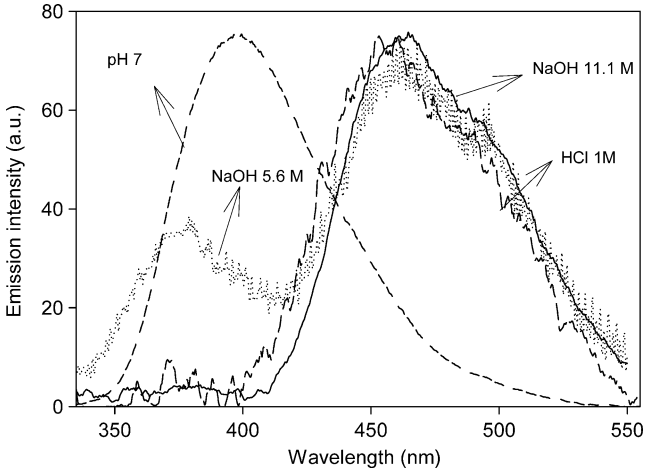

Fig. 9 Normalized fluorescence spectra of representative aqueous AC solutions

in these clusters provides, on the one hand, the proton wires for the sequential hoping of the protons via a Grotthuss like process [35] and, on the other hand, it modulates the proton transfer reaction modifying the strength of the substrate-water hydrogen bonding interactions.

Thus, as we have recently shown in a theoretical study on the hydrogen bond donor capability and co-operative effects in the hydrogen bond complexes of some betacarboline derivatives [36], the strength of the hydrogen bonds can be changed by changing not only the donor nature, but also by increasing the number of donor molecules involved in the hydrogen bond. Concretely, these studies showed that the specific solvation of a hydrogen bonded donor molecule by extra donor molecules can vary the geometry of the hydrogen bond and, consequently, the relative position of the hydrogen atom along the region between the two electronegative centres. Also, it has been recently reported that cooperative hydrogen bonding interactions among water molecules play a key role in the ESDPT of the cyclic 7AI-water complex [9].

Evidently, the rigorous interpretation, at the molecular level, of the influence that the acid/base properties of the aqueous media could have in the hydration shell of the AC molecules is out of the scope of this paper. However, on the basis of the above reasoning, it is reasonable to suspect that the distinct spectroscopic characteristics of the differently hydrated neutral AC species must be related with the modifications that these hydration changes induce in the strengths of the AC-water hydrogen bonding interactions. Thus, in the moderate acid and basic aqueous media there are, as in the water-rich organic-water mixtures, enough water molecules to strongly solvate the neutral AC molecules. Consequently, the cooperative hydrogen bond among the water molecules in these highly solvated species strengthens the AC-water hydrogen bonding interactions, which, in turns, stabilizes the hydrates and diminishes the energy of their spectroscopic transitions. The different magnitudes of the red shifts observed in the absorption and fluorescence spectra of AC upon the formation of these poly hydrates indicate that the strengthening of the AC-water hydrogen bonds is greater in the excited than in the ground state. Conversely, in the concentrated NaOH solutions, the strong solvation of the hydroxide anions considerably reduces the water molecules available for the AC solvation giving place to a primary hydration shell similar to that of the AC molecules in the organic-water mixtures of low water content.

Finally, once the different prototropic species of AC have been spectroscopically characterized, we can estimate their excited state pK_as by using the Förster-Weller method [37]. Thus, assuming the entropies of protonation in the ground and the excited states identical, the pK_a difference between the ground and the lowest excited state, ΔpKa, may be estimated from the steady-state absorption or emission spectra using the following equation:

$$\Delta\mathrm{pKa} = \mathrm{pKa} - \mathrm{pKa}^{*} = \frac{\mathrm{N_A h}}{2.303\ \mathrm{R\ T}}(\nu_{\mathrm{base}} - \nu_{\mathrm{acid}}) = 0.0021(\nu_{\mathrm{base}} - \nu_{\mathrm{acid}}) \quad (8)$$

In this equation, NA is the Avogadro's number, h is the Planck's constant, R is the universal gas constant, T is the absolute temperature, and ν is the frequency of radiation involved in the transition from the ground to lowest excited state of the acid, ν_{acid}, and base, ν_{base}, conjugate pair. To carry out the ΔpKa calculations we have considered that, as the spectral data suggest, the deprotonation of C gives the neutral AC poly-hydrate, N_p, whereas the A species are formed by deprotonation of the neutral AC di-hydrate, N_d. Moreover, because of their similar excitation spectra, we have supposed that these neutral AC hydrates have similar absorption spectra. Thus, using the mean of the absorption

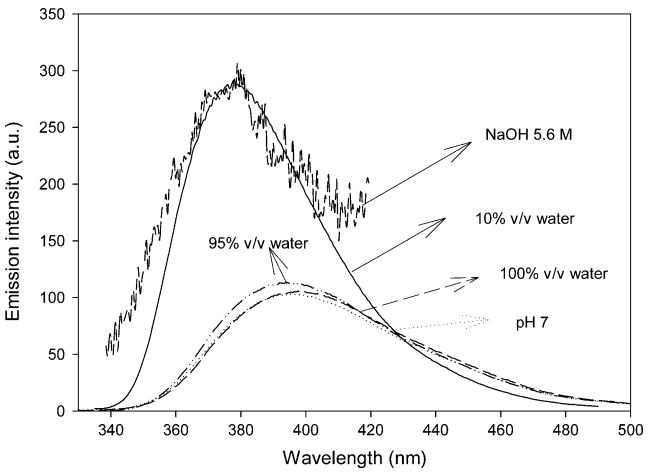

Fig. 10 Comparison among the emissions of AC in selected THF-water mixtures and aqueous solutions

and emission wavelengths to estimate the frequencies ν_{Nd}= 28,682 cm^{-1}, ν_{Np}=27,979 cm^{-1}, ν_C=25,575 cm^{-1} and ν_A= 24,266 cm^{-1} the ΔpKas values of −5.0, and+9.3 for C→N_p, and N_d→A equilibria, respectively, have been obtained. Using a similar approach, Waluk et al. [13] calculated ΔpKa values of −7.5 and +10.8 for the C→N and N→A equilibria, respectively. However, since these authors did not consider the existence of two different neutral species, these data cannot be directly compared with our data.

According to the Förster-Weller cycle analysis, the pyrrolic proton and the pyridine nitrogen atom of AC become, upon light absorption, more acid and more basic, respectively. This behavior is the expected as compared with related compounds as 7AI [7] and other carboline isomers [38]. Thus, with respect to the pyridinic nitrogen atom, AC behaves as pyridinium and isoquinolinium cations [39], whereas for pyrrolic deprotonation it behaves as indole or carbazole [40–42]. Therefore, both the pyridinic and the indolic moieties retain in part their individual characteristics after anellation into the AC skeleton.

Conclusions

The progressive addition of water sequentially changes the absorption and fluorescence spectra of the AC solutions in DX, THF and DEE. These changes have been attributed to the formation, at low water concentrations, of a weakly fluorescent ground state hydrogen bonded AC/$(H_2O)_2$ complex that, further, at higher water concentrations evolves to a highly aggregated AC/water poly hydrate. Since the long wavelength emission around 500 nm, typical of the AC phototautomer, is not observed in the fluorescence spectra of these AC organic solvent-water solutions, we conclude that, unlike 7AI, AC does not form the easily phototautomerizable 1:1 AC/water cyclic complex.

The changes of the absorption spectra of AC in acid/base aqueous solutions indicate the ground state equilibria between the cationic, neutral and anionic prototropic species of AC depicted in Scheme 1. The analysis of the AC fluorescence spectra in the acid/base aqueous solutions reveals the existence of four different excited state AC species: the cationic and anionic species and the two differently hydrated species of the neutral AC previously observed in the organic solvent-water mixtures. The pK_a difference between the ground and lowest excited state, calculated by using the Förster-Weller cycle, indicates that AC becomes much more basic (pyridinic protonation) and much more acid (pyrrolic deprotonation) in the excited than in the ground state.

Acknowledgements We acknowledge financial support from the Junta de Andalucía, 2009/FQM-106.

References

1. Waluk J (2000) Conformational aspects of intra- and intermolecular excited-state proton transfer. In: Waluck J (ed) Conformational analysis of molecules in excited states. Wiley-VCH, New York, pp 57–111
2. Cheng-Chih H, Chang-Ming J, Chou Pi-Tai (2011) Excited proton transfer via hydrogen-bonded dimers and complexes in condensed phase. In: Ke-Li H, Guang-Jiu Z (eds) Hydrogen bonding and transfer in the excited state, Wiley, vol. II, pp. 555–578
3. Avouris P, Yang LL, El-Bayoumi MA (1976) Excited state interactions of 7-azaindole with alcohol and water. Photochem Photobiol 24:211–216
4. Negrerie M, Gai F, Bellefeuille SM, Petrich JM (1991) Photophysics of a novel optical probe: 7-azaindole. J Phys Chem 95:8663–8670
5. Pi-Tai C, Martinez ML, Cooper WC, Collins ST, McMorrow DP, Kasha M (1992) Monohydrate catalysis of excited-state double-proton transfer in 7-azaindole. J Phys Chem 96:5203–5205
6. Collins ST (1983) Exciplex formation in alcohol and water solutions of 7-zaindole. J Phys Chem 87:3202–3207
7. Chapman CF, Maroncelli M (1992) Excited-state tautomerization of 7-azaindole in water. J Phys Chem 96:8430–8441
8. Chen Y, Rich RL, Gai F, Petrich JW (1993) Fluorescent species of 7-azaindole and 7-azatryptophan in water. J Phys Chem 97:1770–1780
9. Park SY, Jeong H, Jang SJ (2011) Anomalously slow proton transport of a water molecule. J Phys Chem B 115:6023–6031
10. Chang C, Shabestary N, El-Bayoumi MA (1980) Excited-state double proton transfer in 1-azacarbazole hydrogen-bonded dimers. Chem Phys Lett 75:107–109
11. Sepiol J, Wild UP (1982) Excited-state double proton transfer in heterodimers of 1-azacarbazole. Chem Phys Lett 93:204–207
12. Waluk J, Pakula B (1984) Viscosity and temperature effects in excited state double proton transfer: luminescence of 1-azacarbazole dimers in solid-state and solution. J Mol Struct 114:359–362
13. Waluk J, Grabowska A, Pakula B, Sepiol J (1984) Viscosity vs. temperature effects in excited-state double proton transfer. Comparison of 1-azacarbazole with 7-azaindole. J Phys Chem 88:1160–1162
14. Waluk J, Herbich J, Oelkrug D, Uhl S (1986) Excited-state double proton transfer in the solid state: the dimers of 1-azacarbazole. J Phys Chem 90:3866–3868
15. Waluk J, Komorowski SJ, Herbich J (1986) Excited-state double proton transfer in 1-azacarbazole-alcohol complexes. J Phys Chem 90:3868–3871
16. Fuke K, Yabe T, Chiba N, Kohida T, Kaya K (1986) Double-proton-transfer reaction in the excited state of 1-azacarbazole dimer and 1-azacarbazole- 7-azaindole heterodimer studied in supersonic jet. J Phys Chem 90:309–2311
17. Fuke K, Kaya K (1989) Dynamics of double-proton-transfer reaction in the excited-state model hydrogen-bonded base pairs. J Phys Chem 93:614–621
18. Fuke K, Tsukamoto K, Misaizu F, Kaya K (1991) Picosecond measurements of the vibrationally resolved proton-transfer rate of the jet-cooled 1-azacarbazole dimer. J Chem Phys 95:4074–4080
19. Mente S, Maroncelli M (1998) Solvation and the excited-state tautomerization of 7-azaindole and 1-azacarbazole: computer simulations in water and alcohol solvents. J Phys Chem 102:3860–3878
20. Catalán J (2007) Photophysics of 1-azacarbazole dimers: a reappraisal. J Phys Chem A 111:8774–8779
21. Angulo G, Carmona C, Pappalardo R, Muñoz MA, Guardado P, Sánchez-Marcos E, Balón M (1997) An experimental and theoretical study on the prototropic equilibria of the four carboline isomers. J Org Chem 62:5104–5109

22. Stephenson L, Warburton WK (1970) Synthesis of some substituted α-carbolines. J Chem Soc C 1355–1364
23. Perkampus HH (1992) UV–VIS spectroscopy and its applications. Springer, Berlin
24. Bagno G, Scorrano G, More O'Ferral RA (1987) Stability and solvation of organic cations. Rev Chem Intermed 7:313–352
25. del Valle JC, Kasha M, Catalán J (2000) The singular coincidence of fluorescence spectra of the anionic and cationic species formed by the respective deprotonated and protonated pyrido-pyrrolo bases. Int J Quant Chem 77:118–127
26. Sánchez Coronilla A, Carmona C, Muñoz MA, Balón M (2009) Ground and singlet excited state pyridinic protonation of N9-methylbetacarboline in water-N, N-dimethylformamide mixtures. J Fluorescence 19:1025–1035
27. Sánchez Coronilla A, Carmona C, Muñoz MA, Balón M (2010) Singlet excited state pyridinic deprotonation of the N_9-methylbetacarboline cations in aqueous sodium hydroxide solutions. J Fluorescence 20:163–170
28. Lee J, Robinson GW, Webb SP, Philips LA, Clark JH (1986) Hydration dynamics of protons from photon initiated acids. J Am Chem Soc 108:6538–6542
29. Robinson GW, Thidthethwhite PJ, Lee J (1986) Molecular aspects of ionic hydration reactions. J Phys Chem 90:4224–4233
30. Lee J, Griffin RD, Robinson GW (1985) 2-naphthol: a simple example of proton transfer affected by water structure. J Chem Phys 82:4920–4925
31. Solntsev KM, Huppert D, Agmon N, Tolbert LM (2000) Photochemistry of "super" photoacids. 2. Excited-state proton transfer in methanol/water mixtures. J Phys Chem A 104:4658–4669
32. Agmon N (2005) Elementary steps in excited-state proton transfer. J Phys Chem A 109:13–35
33. Mohammed OF, Pines D, Dreyer J, Pines E, Nibbering ET (2005) Sequential proton transfer through water bridges in acid base reactions. Science 310:83–86
34. Siwick BJ, Bakker HJ (2007) On the role of water in intermolecular proton-transfer reactions. J Am Chem Soc 129:13412–13420
35. de Grotthuss CJT (1806) Sur la décomposition de l'eau et des corps qu'elle tient en dissolution à l'aide de l'électricité galvanique. Ann Chim 58:54–73
36. Sánchez-Coronilla A, Balon M, Sánchez-Marcos E, Muñoz MA, Carmona C (2010) A theoretical study of the hydrogen bond donor capability and co-operative effects in the hydrogen bond complexes of the diaza-aromatic betacarbolines. Phys Chem Chem Phys 12:5276–5284
37. Valeur B (2002) Molecular fluorescence: principles and applications. Wiley-VCH, Weinheim
38. Balón M, Hidalgo J, Guardado P, Muñoz MA, Carmona C (1993) Acid–base and spectral properties of β-carbolines. Part 2. Dehydro and fully aromatic β-carbolines. J Chem Soc Perkin Trans 2:99–104
39. Vander Donckt E (1970) Acid–base properties of excited states. Progr React Kinet 5:273–299
40. Vander Donckt E (1969) Fluorescence solvent shifts and singlet excited state pKs of indole derivatives. Bull Soc Chim Belg 78:69–75
41. Hidalgo J, Carmona C, Muñoz MA, Balón M (1990) Acid–base properties of carbazole in the ground and lowest excited singlet states. J Chim Phys 87:555–564
42. Balón M, Carmona C, Muñoz MA, Hidalgo J (1989) The acid–base properties of pyrrole an its benzologs indole and carbazole: a re-examination from the excess acidity method. Tetrahedron 45:7501–7504